



IJRASET

International Journal For Research in
Applied Science and Engineering Technology



INTERNATIONAL JOURNAL FOR RESEARCH

IN APPLIED SCIENCE & ENGINEERING TECHNOLOGY

Volume: 7 Issue: X Month of publication: October 2019

DOI: <http://doi.org/10.22214/ijraset.2019.10090>

www.ijraset.com

Call:  08813907089

E-mail ID: ijraset@gmail.com

Non-Stoichiometric Synthesis of Lanthanum Zirconate by Glycine Nitrate Process with Lanthana as Excess Agent

Abhinay Rajput¹, Meenu Srivastava², RPS Chakradhar³, Parthasarathi Bera⁴

¹M.Tech Student, Mechanical Engineering Department, NIT Calicut, Calicut, Kerala-673601, India.

²Principal Scientist, Surface Engineering Division, CSIR-National Aerospace Laboratories, Bangalore, Karnataka-560017, India.

³Scientist, Surface Engineering Division, CSIR-National Aerospace Laboratories, Bangalore, Karnataka-560017, India.

⁴Senior Scientist, Surface Engineering Division, CSIR-National Aerospace Laboratories, Bangalore, Karnataka-560017, India.

Abstract: For top coat of thermal barrier coatings, ceramics with structure type $A_2B_2O_7$ or pyroclore type structure are new line of substances expected to show good thermal properties. So, for that purpose this powder was indigenously prepared in CSIR-NAL. For synthesis of $La_2Zr_2O_7$ powder glycine nitrate method was employed. Synthesized powder has non-stoichiometric addition with excess of lanthana (La_2O_3) to act as dispersoid.

Synthesized powder had surface area to volume ratio. XRD plots showed that after calcination of the as-synthesized powder, phase transition occurs from fluorite to pyroclore. FESEM micrograph showed the agglomeration nature of the as-synthesized powder. Particle size of the as-synthesized powder was 4 microns, which increased to 18 microns post-spray drying. CTE values of the synthesized powder is showing average magnitude of $11.76 \times 10^{-6}/^{\circ}C$ above $600^{\circ}C$. Thermal gravimetric analysis (TGA) showed steep drop down behavior due to release of trapped gases, which then attain stability due to initiation of pyroclore phase formation.

Keywords: pyroclore, glycine, lanthana, dispersoid, fluorite, XRD, FESEM, CTE, TGA

I. INTRODUCTION

It is always desired to increase the thermal life of the turbine blade and combustion chamber components by surface modification with methods like TBC coating, heat treatment, etc. [1],[2]. Coating methods like thermal spraying by plasma vapor disposition, high velocity oxy-fuel methods employed high temperature resistant ceramic coating of materials like $ZrO_2-Y_2O_3$. But due to phase unstablility of zirconia crystal structure at high temperature ($>1200^{\circ}C$) [3]-[5], a new line of materials has been researched from last decade, one of those materials is lanthanum zirconate ($La_2Zr_2O_7$).

Lanthanum zirconate is known for their phase stability at high temperature. It possesses pyroclore structure at temperature greater than $1000^{\circ}C$. Synthesisation of $La_2Zr_2O_7$ can be done by methods like sol gel, hydrothermal, solid state reaction, etc [6]-[9]. Solid state reaction by plasma processing yields this powder in pyroclore structure. Which is difficult by other methods as reaction temperature never reaches beyond $1000^{\circ}C$ and yields only fluorite structure. Glycine nitrate synthesis is one of those methods to produce this powder.

By this method nitrate solutions of the concerned metal nitrates are mixed in certain proportions along with suitable oxidizer like glycine, urea [5]. It forms a glycine-metal complex compound, which is then heated at the combustion temperature of oxidizer to initiate the self-propelling reaction which causes reduction of the nitrate salts of the solution and leaving the ash of the oxide ceramic powder desired [9].

The pryroclore structure of $La_2Zr_2O_7$ can be obtained upon subsequent calcination. This method produces a powder of higher surface area to volume ratio of, which is highly porous, and nanoscale size of powder is produced, with less density. By this method, lowest residual carbon is obtained after reaction completion. Coefficient of thermal expansion (CTE) is lesser as compared to YSZ used in currently used in TBC coatings [10], [11]. Which can cause a mismatch of CTE with that of bond coat resulting in spalling of coating in thermal cycling tests. It is usually doped with other elements like rare earths and transition metals to increase its CTE [12], [13].

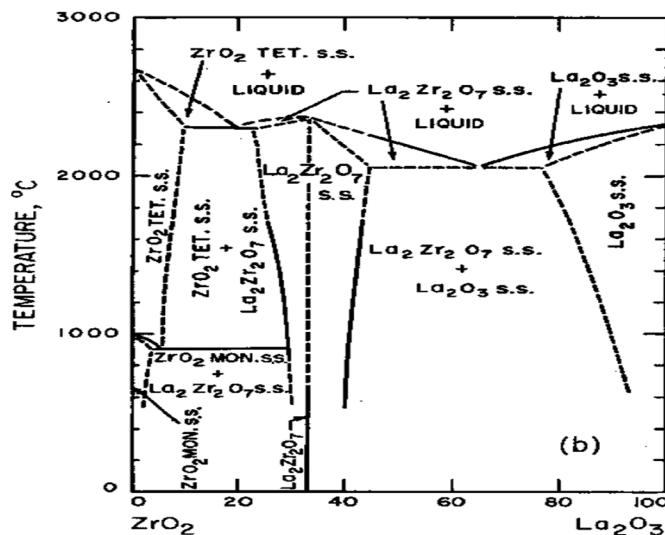


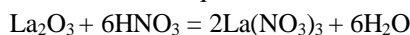
Fig. 1.1. Phase Diagram of lanthana (La₂O₃) and zirconia(ZrO₂) in mole% composition [14].

CTE of lanthanum zirconate can also be increased by presence of other chemically compatible ceramic powder in a composite form [3]. Both the parent ceramic materials of lanthanum zirconate i.e. lanthana (La₂O₃) and zirconia (ZrO₂) has chemical compatibility with lanthanum zirconate as evident from the phase diagram (fig.1.1), lanthana has larger compatibility zone as compared to zirconia in terms of composition as well as temperature. So, combination of lanthana with lanthanum zirconate could provide the properties desirable for top coat of thermal barrier coating.

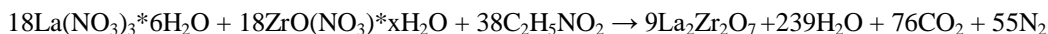
II. MATERIALS AND METHODOLOGY

A. Powder Synthesis

For preparation of the above powder nitrate salts of the zirconium and lanthanum are required. Commercially available lanthanum oxide (La₂O₃), zirconium nitrate (ZrO(NO₃)₃.xH₂O) and glycine (C₂H₅NO₂) of Sigma Aldrich 99% purity were used. Firstly lanthanum nitrate was produced by reacting lanthanum oxide solution with nitric acid to get lanthanum nitrate by slow heating at 60°-70° C at 6 hours to get pale yellow solution. Stoichiometric equation of the solution is:



As the concentration of the HNO₃ used here was 69% so it was compensated by adding extra HNO₃ to match the stoichiometric composition. Then the separately prepared solutions of zirconium nitrate and glycine are mixed and stirred well, a translucent white solution has been obtained. It is then heated at 400°C in a closed furnace. After the evaporation of excess water, white foam will emerge from the liquid vapor interface with evolution of gases of carbon dioxide and nitrogen. The concerned stoichiometric reaction is:



It is worth mentioning that water of crystallization has to be considered while balancing the equation to take the required weight of chemicals while reaction, neglecting water of crystallization causes lanthanum nitrate to become limiting reagent and foam changes colour (white→pale yellow→peach). 10% excess of stoichiometric amount of lanthanum nitrate is taken in the reaction for zirconium nitrate's water of crystallization, x is taken as 2.

B. Powder Processing

- 1) *Hand Milling:* As-synthesised powder foam has very high surface area to volume with gases (CO₂ and N₂) trapped in it. It was milled in motor piston to provide evolve trapped gases and decrease its volume for handling purpose.
- 2) *Calcination:* As-obtained powder was steadily heated in normal atmosphere from room temperature to 1000°C and 1200°C and maintained at that temperature for 5 hours. It was then cooled down to room temperature through furnace cooling. Powder was heated in alumina cup to maintain powder inertness with the container.
- 3) *Spray Drying:* For spheroidization of powder particles, spray drying was done with the aqueous solution of calcined lanthanum zirconate powder. 6% vol. of polyvinyl alcohol was added in the aqueous slurry. Slurry feed rate of 3 RPM was fed into dryer chamber at 6 bar pressure and 200°C



Fig. 2.1. Spray Drying of as-synthesised calcined lanthanum zirconate powder. (Property of CSIR-NAL Bangalore)

C. Characterisation of Synthesized Powder

The surface morphology and composition of the as-synthesized and spray dried powders were analyzed using field emission scanning electron microscope (FESEM) affixed with energy dispersive spectrometer (EDAX) respectively. The phase identification was done by X-ray diffractometer (Bruker D8) using $\text{CuK}\alpha$ radiation of wavelength 0.154 nm. Thermal expansion analysis was done using NETZSCH DIL 402CL DIL402CLA-0127-L for as-synthesised powder sample of length 7.131m and cross-section of 28.94 mm^2 . Sample heated in controlled air from 26°C to 1100°C with uniform heating and cooling rate $10\text{K}/\text{min}$. Holding time for sample at 1100°C was 1 hour. Thermal gravimetric analysis of the powder sample was done in SENSYS EVO under controlled oxygen supply from 50°C to 830°C .

III. RESULT AND DISCUSSION

From FESEM results, as-synthesized $\text{La}_2\text{Zr}_2\text{O}_7$ powder is in agglomerated form in a sponge like appearance. From the FESEM micrographs of dispersed powder, the powder particles exists in morphologies of spherical and columnar shape linked together in chains. Particle size of as-synthesized powder ranges from $4\mu\text{m}$ to fractions of microns.

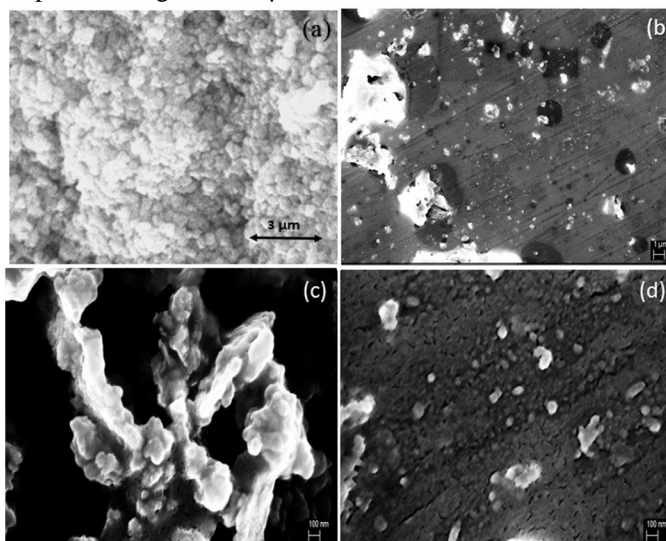
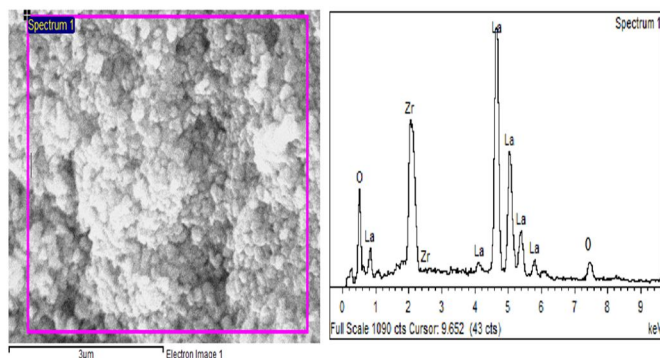


Fig. 3.1. FESEM micrographs of the as-synthesized $\text{La}_2\text{Zr}_2\text{O}_7$ powder in agglomerated state (a, c) and dispersed state (b, d)

EDAX analysis gives lanthanum in maximum weight% followed by oxygen and zirconia. It indicates the presence of excess lanthanum oxide than stoichiometric after the powder synthesis. It is deliberately taken in excess so that it would completely combine zirconia in the reaction stage. Also, it slightly increases the thermal conductivity of the lanthanum zirconate for the purpose of which it has been synthesized.



Element	Weight%	Atomic%
Oxygen	17.73	57.84
Zirconium	18.09	12.66
Lanthanum	64.18	29.50

Fig. 3.2.; Table. 3.1. EDAX analysis of the as-synthesized $\text{La}_2\text{Zr}_2\text{O}_7$ powder

XRD confirms the presence of lanthanum oxide alongside the high intensity peaks of lanthanum zirconate. In as synthesized powder lanthanum zirconate is present in fluorite form (JCPDS 71-2623) evident from peaks of (222), (440), (400) and (622). There is increase in peak intensity upon calcination in 1000°C and 1200°C . Also there is change in phase of lanthanum zirconate from fluorite to pyrochlore (JCPDS 73-0444) structure with the emergence of new peaks of (266), (444), (840). It also indicates that the as-synthesized powder has amorphous phases, which upon heating restructured itself to yield pyrochlore structure [15].

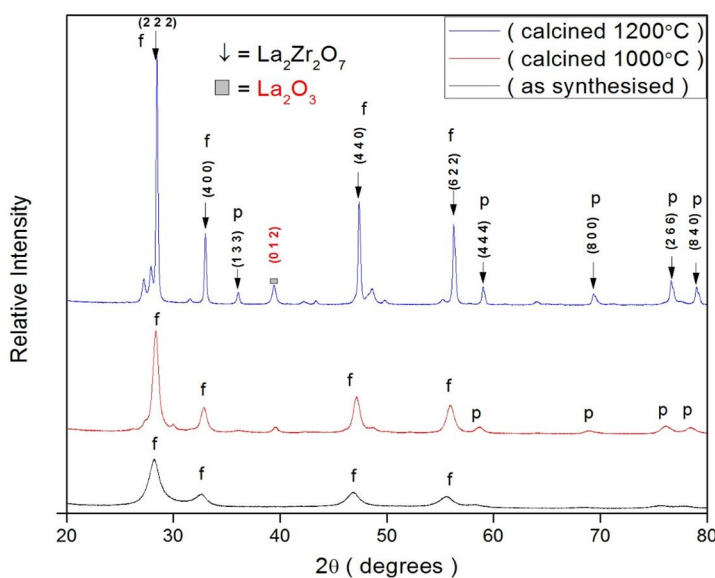


Fig. 3.3. XRD comparison of as-synthesized and calcined powders of $\text{La}_2\text{Zr}_2\text{O}_7$.

By scherrer formula crystallite size of particles was evaluated corresponding to highest peak in the XRD diffractogram. Crystallite sizes are shown in table 2.1. With increase in calcination temperature, increase in crystallite size has been observed.

Sample	Crystallite Size
As-synthesized	5.46 nm
1000°C calcined	12 nm
1200°C calcined	38.41 nm

Table. 3.2. Crystallite size of $\text{La}_2\text{Zr}_2\text{O}_7$ powder after synthesis and calcination

Taking account of TGA analysis of the as-synthesized sample (fig 3.4), powder weight showed steep decline (shallow step exothermic peaks) around temperature of 200-220°C owing to the escape of trapped gases of CO_2 , N_2 and moisture. From 220-410°C, the powder weight showed the gradual decreasing stepped slope (shallow step exothermic peaks) attributing to the further volatility of the structural water (water of crystallization) [15]. Increasing the temperature till 700°C showed no signs of weight change due to stability regime of fluorite phase of $\text{La}_2\text{Zr}_2\text{O}_7$. Beyond 700°C, there is a slight increase of weight depicted by peaks at 855, 875 and 898°C (shallow step endothermic peaks) showing the initiation of phase change from fluorite to pyrochlore structure.

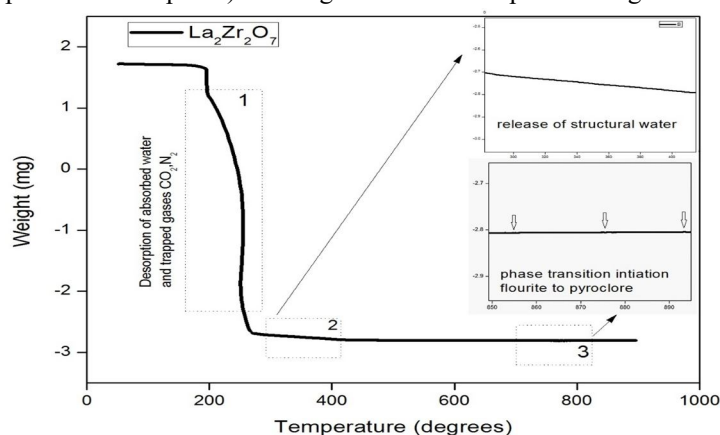


Fig 3.4 TGA curve of the as-synthesized $\text{La}_2\text{Zr}_2\text{O}_7$ powder in controlled supply of O_2

Observation of the thermal expansion curve (fig 3.4) of as-synthesized $\text{La}_2\text{Zr}_2\text{O}_7$ powder are in sync with the TGA results. There is a slight non-uniformity observed in linear strain all over the operating temperature, owing to the presence of La_2O_3 in the as-synthesized $\text{La}_2\text{Zr}_2\text{O}_7$ powder. Linear strain showed steep slope from 300-500°C, probably due to internal vibration exerted by trapped gases and moisture causing longitudinal/transverse motion causing powder molded specimen to expand. After release of trapped gases and moisture it started to compress down mildly beyond 600°C due to the crystal lattice contraction because of increased intensity of heavy metal ions and transition metal ions (La^{3+} and Zr^{4+}) in transverse direction. A shallow peak around 900°C marks the initiation of change of phase from fluorite to pyrochlore. Average value evaluated for coefficient of thermal expansion from 500-1000°C is $11.76 \times 10^{-6} / ^\circ\text{C}$, which is slightly more than the reported values [15], [16]. From the SEM/EDAX analysis of $\text{La}_2\text{Zr}_2\text{O}_7$ powder post spray drying the powder particles aggregated to form spherical shape. The macro-particle has partially visible grain boundaries separating the smaller particles. The macro-particle size thus obtained is 18-20µm.

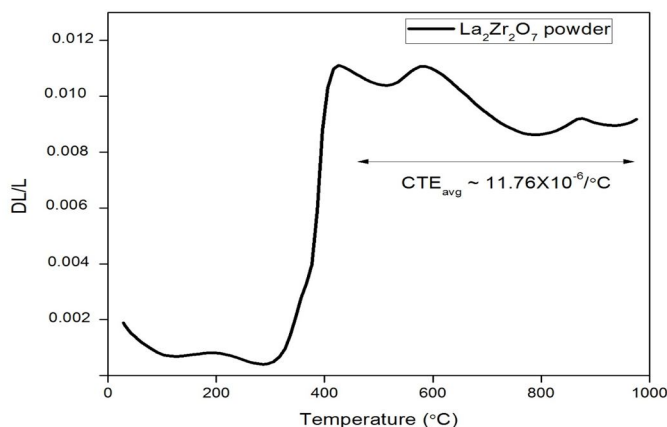
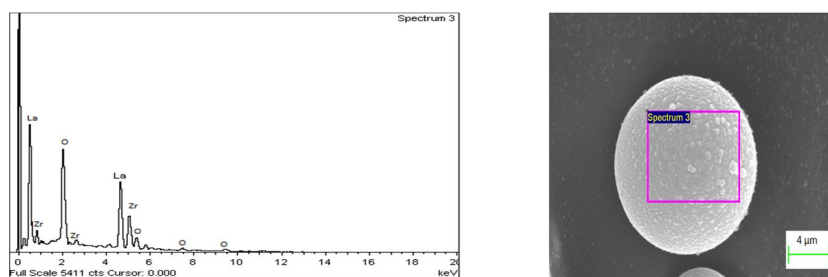


Fig. 3.5. Thermal expansion curve of as-synthesized $\text{La}_2\text{Zr}_2\text{O}_7$ powder in controlled supply of air.



Element	Weight%	Atomic%
Oxygen	18.82	59.67
Zirconium	19.31	13.25
Lanthanum	61.87	27.08

Fig. 3.6.; Table 3.3. FESEM/EDAX analysis of $\text{La}_2\text{Zr}_2\text{O}_7$ powder post calcination and spray drying.

There are negligible changes in the element compositions post spray drying. For the purpose of thermal spraying of these powders, there is requirement of the free-flowing of spray powder. Also, there is a particle size restraint needed in thermal spray processes. Powder processing by spray drying makes it ready for thermal spray operations.

IV. CONCLUSION

Synthesization by glycine nitrate process has yielded physically indistinguishable chemically compatible powder of lanthanum zirconate ($\text{La}_2\text{Zr}_2\text{O}_7$) and lanthana (La_2O_3) with lanthanum zirconate in major proportion. The synthesized powder has high surface area to volume ratio. FESEM micrograph showed the formation of powder particles in spherical as well as columnar shape with average size of 4 microns. From TGA analysis, the powder underwent the loss of mass due to release of trapped gases, moisture and release of structural water before showing stability at high temperatures. Similarly, thermal expansion showed increase in tensile strain in powder molded sample followed by stability beyond 600°C . XRD diffractogram showed the formation of fluorite phase of lanthanum zirconate. Upon calcination above 1000°C , powder showed the peaks formation of pyrochlore phase, which reflects the stable regime in TGA and thermal expansion curve. Presence of lanthana in the powder slightly increases the CTE of lanthanum zirconate from the reported values. Spray drying of the powder changes the particles shape into spherical by agglomeration of smaller particles increasing its size to 18 microns.

V. ACKNOWLEDGEMENT

The authors would like to thank Director, NAL, and Head, SED for their support and encouragement. The authors express their gratitude to Dr. Sheela Singh of SRM University Chennai, INDIA for providing thermal expansion results for the synthesized powder. Authors would like to extend their thanks to Mr. Siju, Mr. praveen, Mr. Srinivas for their assistance rendered in the characterization of the synthesized powder.

REFERENCES

- [1] Clarke, D.R., Oechsner, M. and Padture, N.P., 2012. Thermal-barrier coatings for more efficient gas-turbine engines. *MRS bulletin*, 37(10), pp.891-898.
- [2] Clarke, D.R. and Levi, C.G., 2003. Materials design for the next generation thermal barrier coatings. *Annual review of materials research*, 33(1), pp.383-417.
- [3] Ma, W., Gong, S., Xu, H. and Cao, X., 2006. The thermal cycling behavior of Lanthanum-Cerium Oxide thermal barrier coating prepared by EB-PVD. *Surface and Coatings Technology*, 200(16-17), pp.5113-5118.
- [4] Vassen, R., Cao, X., Tietz, F., Basu, D. and Stöver, D., 2000. Zirconates as new materials for thermal barrier coatings. *Journal of the American Ceramic Society*, 83(8), pp.2023-2028.
- [5] Schlichting, K.W., Padture, N.P. and Klemens, P.G., 2001. Thermal conductivity of dense and porous yttria-stabilized zirconia. *Journal of materials science*, 36(12), pp.3003-3010.
- [6] Bolech, M., Cordfunke, E.H.P., Van Genderen, A.C.G., Van Der Laan, R.R., Janssen, F.J.J.G. and Van Miltenburg, J.C., 1997. The heat capacity and derived thermodynamic functions of $\text{La}_2\text{Zr}_2\text{O}_7$ and $\text{Ce}_2\text{Zr}_2\text{O}_7$ from 4 to 1000 K. *Journal of Physics and Chemistry of Solids*, 58(3), pp.433-439.
- [7] Sedmidubský, D., Beneš, O. and Konings, R.J.M., 2005. High temperature heat capacity of $\text{Nd}_2\text{Zr}_2\text{O}_7$ and $\text{La}_2\text{Zr}_2\text{O}_7$ pyrochlores. *The Journal of Chemical Thermodynamics*, 37(10), pp.1098-1103.
- [8] Shimamura, K., Arima, T., Idemitsu, K. and Inagaki, Y., 2007. Thermophysical properties of rare-earth-stabilized zirconia and zirconate pyrochlores as surrogates for actinide-doped zirconia. *International Journal of Thermophysics*, 28(3), pp.1074-1084.



- [9] Chick, L.A., Pederson, L.R., Maupin, G.D., Bates, J.L., Thomas, L.E. and Exarhos, G.J., 1990. Glycine-nitrate combustion synthesis of oxide ceramic powders. *Materials letters*, 10(1-2), pp.6-12.
- [10] Hasselman, D., Johnson, L.F., Bentsen, L.D., SYED, R., Lee, H.L. and SWAIN, M.V., 1987. Thermal diffusivity and conductivity of dense polycrystalline ZrO. *Am. Ceram. Soc. Bull*, 66(5), pp.799-806.
- [11] Cao, X.Q., Vassen, R., Jungen, W., Schwartz, S., Tietz, F. and Stöver, D., 2001. Thermal stability of lanthanum zirconate plasma-sprayed coating. *Journal of the American Ceramic Society*, 84(9), pp.2086-2090.
- [12] Omata, T., Okuda, K., Tsugimoto, S. and Otsuka-Matsuo-Yao, S., 1997. Water and hydrogen evolution properties and protonic conducting behaviors of Ca²⁺-doped La₂Zr₂O₇ with a pyrochlore structure. *Solid State Ionics*, 104(3-4), pp.249-258.
- [13] Omata, T., Ikeda, K., Tokashiki, R. and Otsuka-Yao-Matsuo, S., 2004. Proton solubility for La₂Zr₂O₇ with a pyrochlore structure doped with a series of alkaline-earth ions. *Solid State Ionics*, 167(3-4), pp.389-397.
- [14] Brown Jr, F.H. and Duwez, P.O.L., 1955. The Systems Zirconia-Lanthana and Zirconia-Neodymia. *Journal of the American Ceramic Society*, 38(3), pp.95-101.
- [15] Chen, H., Gao, Y., Liu, Y. and Luo, H., 2009. Coprecipitation synthesis and thermal conductivity of La₂Zr₂O₇. *Journal of Alloys and Compounds*, 480(2), pp.843-848.
- [16] Zhang, J., Guo, X., Jung, Y.G., Li, L. and Knapp, J., 2017. Lanthanum zirconate based thermal barrier coatings: A review. *Surface and Coatings Technology*, 323, pp.18-29.
- [17] Ma, W., Gong, S., Xu, H. and Cao, X., 2006. On improving the phase stability and thermal expansion coefficients of lanthanum cerium oxide solid solutions. *Scripta materialia*, 54(8), pp.1505-1508.



10.22214/IJRASET



45.98



IMPACT FACTOR:
7.129



IMPACT FACTOR:
7.429



INTERNATIONAL JOURNAL FOR RESEARCH

IN APPLIED SCIENCE & ENGINEERING TECHNOLOGY

Call : 08813907089  (24*7 Support on Whatsapp)